IEEE Access
Multidisciplinary | Rapid Review | Open Access Journal

Received November 8, 2019, accepted December 23, 2019, date of publication January 1, 2020, date of current version January 10, 2020.

Digital Object Identifier 10.1109/ACCESS.2019.2963485

Radiation Absorption Noise for Molecular Information Transfer

S. PRATAP SINGH[1], (Member, IEEE), SHEKHAR SINGH[1], WEISI GUO[2], (Senior Member, IEEE), SAKET MISHRA[3], AND SANJAY KUMAR[4]

[1]Galgotias College of Engineering and Technology, Greater Noida 201306, India
[2]Centre for Autonomous and Cyber-Physical Systems, Cranfield University, Cranfield MK43 0AL, U.K.
[3]IBM India Pvt., Ltd., Noida 201301, India
[4]Birla Institute of Technology, Mesra, Ranchi 835215, India

Corresponding author: S. Pratap Singh (drsprataps@gmail.com)

ABSTRACT Molecular signaling is ubiquitous across scales in nature and finds useful applications in precision medicine and heavy industry. Characterizing noise in communication systems is essential to understanding its information capacity. To date, research in molecular nano communication (MNC) primarily considers the molecular dynamics within the medium, where various forms of stochastic effects generate noise. However, in many real-world scenarios, external effects can also influence molecular dynamics and cause noise. Here, the noise due to the temperature fluctuations from incident electromagnetic (EM) radiation is considered, with applications ranging from cell signaling to chemical engineering. EM radiation and subsequent molecular absorption cause temperature fluctuations which affect molecular dynamics and can be considered as an exogenous noise source for MNC. In this paper, the probability density function of the radiation absorption noise (RAN) is analyzed and to demonstrate applicability, we include characteristics of different tissues of the human body. Furthermore, the closed-form expression of error probability (EP) for MNC under the radiation noise is derived. Numerical analysis is demonstrated on different tissues of the human body: skin, brain, and blood, as well as the polarization factor of incident EM radiation is demonstrated. The coupling relationship between the radiation frequency and the intrinsic impedance of the human body on the PDF of radiation absorption noise is presented. This is useful for understanding how mutual information changes with external radiation sources.

INDEX TERMS Molecular communication, noise modeling, and channel modeling.

I. INTRODUCTION

Extreme environments present a significant challenge to conventional wireless signals that are used for monitoring, control, and communications. Such environments include in vivo health monitoring and targeted drug delivery (lossy propagation), adversarial chemical engineering environments (high temperature and radiation), and these form part of the wider Nuclear Biological and Chemical (NBC) defense challenges. With the development of nano-technology, a new communication paradigm known as Nano Communication (NC) presents the aforementioned extreme environments. Fundamentally, NC is based on nanotechnology which comprises of design and production of devices and systems at the atomic and molecular scales (nano-scale). Specifically, NC groups of different Nanoscale components make the integrated functional devices known as nano-machine which achieves all the functionality of the familiar modern communication system. In other words, Nanomachines perform the signal processing tasks like encoding, transmitting, and receiving of the information [1]. Currently, NC is divided into two categories; Molecular Nano Communication (MNC) and Electromagnetic Nano communication (EMNC). MNC is a bio-inspired approach as it is inspired by the natural phenomenon of biology and deals with the emission, propagation, and reception of molecules using Nanomachines (natural/artificial) [2]. EMNC is inspired by miniaturization of communication devices and deals with transmission propagation and reception of EM waves radiated by some novel nanodevice in the Terahertz band [3], [4].

Further, the literature reveals that MNC, EMNC, and traditional microwave communication coexist in some typical multiple access technology scenarios [5]. In other applications, external EM radiation is used to heat the

The associate editor coordinating the review of this manuscript and approving it for publication was Jenny Mahoney.

This work is licensed under a Creative Commons Attribution 4.0 License. For more information, see http://creativecommons.org/licenses/by/4.0/

medium or influence a process. In such scenarios, an increase in temperature due to the absorption of EM energy by molecules results in radiation absorption noise in MNC [4]–[7].

Noise sources in MNC originate intrinsically differently than for noise sources in EMNC [9]. So, the rest of this section presents various literature which includes noise modeling and its analysis with respect to MNC.

The design of a unicast and broadcast MNC is analyzed under different noise reduction approaches namely, F (noise-free), N (all-noise), E (exponential decay) and R (receiver removal) [10]. In the case of diffusion-based communication for low noise regimes, F and N approaches have the same information rate but it is reduced for E and R approaches. While in the case of hybrid-aster F, E, N has a low noise level with nearly similar information rate but for R the information rate is very low [10]. Additive inverse Gaussian noise (AIGN) is proposed in [11] for MNC over fluid medium as a propagation channel. Symbol Error Probability (SEP) with t-ary modulation for different values of t is analyzed under AIGN noise. The different filter techniques such as average filtering and maximum likelihood (ML) detection are used to improve the performance of MNC under AIGN noise [11]. Also, in [12] noise from multiple sources over fluid medium is proposed for MNC as an extension of reaction-diffusion master equation (RDMEX) with exogenous input. The effect of analytical noise in Particulate Drug Delivery Systems (PDDS) over a cardiovascular channel of MNC is presented in [6]. It includes all the noise effects that affect the injection, propagation, and reception of drug nanoparticles. Drug reception probability is proposed in terms of various parameters including blood temperature. Finally, the effect of, blood vessel dimensions, diffusion coefficient, and blood velocity respectively on capacity is analyzed [6].

In [7], the analysis of the information rate for EMNC is presented by considering the additive colored Gaussian distribution as the molecular absorption noise. Authors, in [13] presents the effects of the temperature variations inside the human body on the capacity of diffusion-based MNC. It is found that as concentration decreases with an increase in temperature, theoretic capacity increases. The effect of temperature in the modeling of the molecular channel is analyzed in [14]. Perhaps for the first time authors in [14] have presented fading distributions, the joint distribution of the channel gain and additive noise and its effect on intersymbol interference (ISI) with experimental data validation. As an important observation, it is noted that only the standard deviation of the temperature variations strongly affects the ISI distribution. It is noteworthy to mention that though Specific Absorption Rate (SAR) of EM radiation is studied in various literature [15], [16] demonstrating different thermal effects of it on human body tissues. However, the authors in [4], [17] introduces the effect of EM radiation as the noise may be termed as RAN. Closed-form expressions for the rise in temperature due to the absorption of EM energy have been proposed in [4] for both single-particle and multiple particle scenarios. It also proposes expressions for an increase in temperature used for the analysis of the molecular absorption power at the receiver [4]. But, it considers the homogeneous medium of propagation which is an oversimplified assumption. Moreover, it has taken only single tissue (blood) as an example of a homogeneous medium for numerical analysis purposes. While, authors in [17] have analysed spectral radiance and power spectral density thoroughly. The propagation of EM waves inside the human body is severely impacted by the absorption of liquid water molecules [18]. In vivo communication, the power spectral density as a function of distance and frequency is calculated in [19], while channel capacity and transmission range are calculated in [20] both under the molecular absorption noise. Though, authors in [8] analyses the effect of molecular absorption noise which has been carried out for different tissues of the human body such as fat, blood, skin, etc., but from EMNC point of view. For EMNC they concluded that with an increase in the distance between transmitter and receiver the level of received information decreases as the noise level increases due to molecular absorption in the medium.

It is noticeable that as per the authors' best knowledge, to date, none of the literature has presented analytical expressions of the RAN as function of temperature due to the absorption of EM energy by the molecules of the medium and its effect on Molecular information transfer (MIT). So, this paper explores the aforesaid issues. The analysis is made at different frequency range, for the human body as a demonstration of applicability, considering different tissue of the human body like skin, blood, and brain [21]. However, following are the major technical contributions of the manuscripts:

1) The statistical model of the noise, termed as radiation absorption noise (RAN), due to increase in temperature by virtue of incident EM is proposed for contemporary molecular communication.
2) Novel closed form expression for the PDF of the proposed RAN is presented which includes the impedance of the human body tissues (skin, brain, and blood), the polarization factor of incident and frequency of incident EM wave.
3) Novel closed form expression for the Error Probability (EP) under of the proposed RAN is derived to quantify the performance of molecular communication.
4) Presents thorough demonstration on the effects of tissues of the human body (skin, brain, and blood), the polarization factor of incident EM radiation and the coupling relationship between the radiation frequency and the intrinsic impedance of the human body.

The rest of the paper is organized as follows. In Sec. II, the probability density function of radiation absorption noise as a function of temperature and error probability is formulated. In Sec. III, the numerical analysis has been made at different frequencies for different human body tissues and the polarization factor effects have been discussed and finally, the conclusion has been made in Sec. IV.

II. PROPOSED RADIATION ABSORPTION NOISE (RAN) AND ERROR PROBABILITY (EP) FOR MNC

In MNC, molecular absorption noise is composed of the channel environment noise, the self-induced noise, and the molecular absorption of the transmitted signal [22]. However, noise due to the increase in temperature by virtue of incident EM energy on tissues of the body should be an additional source of noise in MNC [4]. This section proposes radiation absorption noise due to this increase in temperature: expressions of PDF of RAN and EP under the RAN are derived. First of all, Stefan-Boltzmann (SB) law [23] and power density of EM waves are used to find a relation between radiation and energy and then [24] is used to derive the PDF of RAN in terms of temperature. Next, an analytical expression for EP is derived using the PDF of RAN.

A. PDF OF RAN

According to Stefan-Boltzmann Law [23], the thermal energy radiated by a body radiator is proportional to the fourth power of the absolute temperature and is given by

$$P = A\epsilon\sigma T^4 \tag{1}$$

where, P (in *Watt*) is the Power, A (in m^2) is the surface Area, ϵ is the emissivity of the body, σ is the Stefan-Boltzmann Constant ($Wm^{-2}K^{-4}$) and T (in K) is the temperature of the body. Now, Eq. (1) can be rewritten as

$$\frac{P}{A} = \epsilon\sigma T^4 \tag{2}$$

Again, power density of EM wave can be given as

$$\frac{P}{A} = \frac{E_0^2}{2\eta} \tag{3}$$

where, E_0 (in V/m) is the peak of electric field intensity and η (in Ω) is intrinsic impedance of the body tissue. But according to [4], molecules in the human body absorb EM energy and subsequently release this energy as heat to their immediate surroundings which in turn causes rise in temperature. So, from Eq. (2) and Eq. (3) we can write

$$\frac{E_0^2}{2\eta} = \epsilon\sigma T^4 \tag{4}$$

though, in Eq. (3) E_0 is the peak of electric field intensity. However, as Eq. (4) establishes the relation between E_0 and temperature (T) [4, 23]. So, without loss of generality we can rewrite Eq. (4) as

$$E_0^2(T) = 2\epsilon\eta\sigma T^4 \tag{5}$$

Eq. (5) shows the relation between electric field intensity, $E_0(T)$ and temperature. It is noteworthy to mention that, the rise in temperature is exogenous noise source for MNC [4]. So, there must be a PDF for this noise, called as PDF of RAN. But, as per our best knowledge none of the literatures present PDF of RAN. Although, PDF of electric field $E_0(T)$ i.e. $f_E(E_0(T))$ is given by [24] and a similar scenario is used to measure and validate the EM absorption for human body in [25], [26]. Hence, without loss of generality PDF $f_E(E_0(T))$ of $E_0(T)$ can be taken as

$$f_E(E_0(T)) = \sum_{n=1}^{3} \frac{2\beta_n}{\alpha_n} \exp(-\epsilon_n(E_0^2(T))) \tag{6}$$

where, n is equal to 1, 2 and 3 for each principal direction respectively and corresponding coefficients, α_n and β_n are as given in [24]:

$$\alpha_1 = \frac{3}{1 + 2P_{13} - P_{23}} \tag{7}$$

$$\beta_1 = \frac{1}{P_{13}(P_{13} - P_{23})} \tag{8}$$

$$\alpha_2 = \frac{3}{1 + 2P_{23} - P_{13}} \tag{9}$$

$$\beta_2 = \frac{1}{P_{23}(P_{23} - P_{13})} \tag{10}$$

$$\alpha_3 = \frac{3}{1 - P_{13} - P_{23}} \tag{11}$$

$$\beta_3 = \frac{1}{P_{13}P_{23}} \tag{12}$$

where, P_{13} and P_{23} are the polarization factors along the two planes.

Following variate transformation can be used in Eq. (6) to derive the PDF of the magnitude of the temperature

$$f_T(T) = f_E(E_0(T))\frac{dE_0(T)}{dT} \tag{13}$$

now, substituting value of $E_0(T)$ from Eq. (5) and value of $f_E(E_0(T))$ form Eq. (6) into Eq. (13), we get

$$f_T(T) = \sum_{n=1}^{3} E_0(T)\frac{2\beta_n}{\alpha_n} \exp\left(-\alpha_n E_0^2(T)\right)\frac{d\sqrt{(2\eta\epsilon\sigma T^4)}}{dT} \tag{14}$$

Eq. (14) can further be simplified as

$$f_T(T) = \sum_{n=1}^{3} 8\eta\epsilon\sigma T^3 \frac{\beta_n}{\alpha_n} \exp(-2\eta\sigma\alpha_n\epsilon T^4) \tag{15}$$

where, T is the temperature, Eq. (15) represents the PDF of radiation absorption noise due to temperature variation in MNC channel. As per authors best knowledge, Eq. (15) is novel and can be used to understand how mutual information changes with external radiation sources in MNC. Further, for numerical analysis of Eq. (15) intrinsic impedance (η) of body tissues can be calculated from [27] for THz (which correspond to EM radiation from EMNC) and [21], [28] for MHz (which correspond to EM radiation from traditional microwave communication) frequency range.

B. ERROR PROBABILITY UNDER RAN

Assuming, H_1 and H_0 be the hypothesises correspond to the transmission of information and no transmission of information respectively. Then, PDF under hypothesis H_0 and H_1 can be represented by $P_{H_0}(T)$ and $P_{H_1}(T)$ respectvely.

Now, without loss of generality, using Eq. (15) with [29], $P_{H_0}(T)$ and $P_{H_1}(T)$ can be given by Eq. (16) and Eq. (17)

$$P_{H_0}(T) = f_T(T) = \sum_{n=1}^{3} 8\eta\epsilon\sigma T^3 \frac{\beta_n}{\alpha_n} \exp(-2\eta\sigma\alpha_n\epsilon T^4) \quad (16)$$

$$P_{H_1}(T) = f_T(T-d) = \sum_{n=1}^{3} 8\eta\epsilon\sigma (T-d)^3 \frac{\beta_n}{\alpha_n} \exp(-2\eta\sigma\alpha_n\epsilon (T-d)^4) \quad (17)$$

where referring to [29], d is the distance between the means of the two densities. Now, without loss of generality, under binary assumption, the probability of successful reception and no reception will be equal i.e. $P_{H_0}(T) = P_{H_1}(T) = 1/2$. Also, it is noticeable that for $P_{H_0}(T) = P_{H_1}(T) = 1/2$ the value of threshold will be *d/2*. Then, the probability of false alarm (P_F) and probability of detection (P_D) can be given by [29]

$$P_F = \int_{d/2}^{\infty} f_T(T)dT \quad (18)$$

$$P_D = \int_{d/2}^{\infty} f_T(T-d)dT \quad (19)$$

Substituting Eq. (16) into Eq. (18) we get

$$P_F = \int_{d/2}^{\infty} \sum_{n=1}^{3} 8\eta\epsilon\sigma T^3 \frac{\beta_n}{\alpha_n} \exp(-2\eta\alpha_n\epsilon\sigma T^4)dT \quad (20)$$

now letting, $u = T^4$ and with simple substitutions, we get

$$P_F = \int_{z}^{\infty} \sum_{n=1}^{3} 2\eta\epsilon\sigma \frac{\beta_n}{\alpha_n} \exp(-2\eta\alpha_n\epsilon\sigma u)du \quad (21)$$

on solving integration in Eq. (21) (which is straight forward) we get probability of false alarm as

$$P_F = \sum_{n=1}^{3} \frac{\beta_n}{\alpha_n} \exp(-2\eta\alpha_n\epsilon\sigma (d/2)^4) \quad (22)$$

now, with Eq. (15), Eq. (17), and Eq. (19) we get

$$P_D = \int_{d/2}^{\infty} \sum_{n=1}^{3} 8\eta\epsilon\sigma (T-d)^3 \frac{\beta_n}{\alpha_n} \exp(-2\eta\alpha_n\epsilon\sigma (T-d)^4)dT \quad (23)$$

again, solving integration in Eq. (23) yields probability of detection as

$$P_D = \sum_{n=1}^{3} \frac{\beta_n}{\alpha_n} \exp(-2\eta\alpha_n\epsilon\sigma (d/2)^4) \quad (24)$$

however, error probability under condition of binary transmission with equal probability, $P_{H_1} = P_{H_2} = 1/2$ (non-equal transmission strategy can be also used which is left as future aspect of this article) can be given by [29]

$$P_e(\xi) = \frac{1}{2}(P_F + P_D) \quad (25)$$

TABLE 1. List of parameters used in simulation.

Symbol	Parameter	Value
σ	Stefan's proportionality constant	5.670373 x 10^3 W m^{-2} K^{-4}
ϵ	Emissivity of the radiating body	0.94 - 0.98
η	Intrinsic Impedance	30 Ω - 67 Ω (MHz frequency range) and 0.090 $M\Omega$ - 0.154 $M\Omega$ (THz frequency range)
P_{13}, P_{23}	Polarization factors	$0 < P_{13}, P_{23} < 1$
S/NT	Signal to Temperature Noise Ratio	in dB

where, from [30, Eq. 5.2.5], without loss of generality ξ represents the signal to temperature noise ratio (S/N_T). Now, substituting P_F from Eq. (22) and P_D form Eq. (24) into Eq. (25) we get final expression of error probability under RAN as

$$P_e(S/N_T) = \sum_{n=1}^{3} \frac{\beta_n}{\alpha_n} \exp(-2\eta\alpha_n\epsilon\sigma (d/2)^4) \quad (26)$$

As per authors best knowledge Eq. (26) is novel and never reported in the literature. However, it is noteworthy to mention that the effect of RAN appears as N_T in Eq. (26). So, more the value of temperature more is the value of noise (N_T) which results in the higher value of EP. The effect of the polarization factor of the incident EM radiation, coupling relationship between the radiation frequency and the intrinsic impedance of the human tissues (skin, blood, brain, muscle) on EP can be examine using Eq. (26).

III. NUMERICAL DISCUSSION

This section presents the numerical evaluation of the analytical expressions proposed due to the increase in temperature by virtue of incident EM energy on the human body tissues. Illustration and understanding of the effects due to intrinsic impedance of the human body tissues (skin, brain, and blood) and polarization factor of incident EM wave, on molecular information transfer of MNC, is presented.

The parameters used for analysis are as follows (also shown in Table 1): Stefan's proportionality constant (σ) is equal to 5.670373 x 10^3 $Wm^{-2}K^{-4}$ [23], intrinsic impedance (η, in Ω) of body tissues (blood, brain, and skin) can be calculated from [27] for THz (which correspond to EM radiation from EMNC) and [21], [28] for MHz (which correspond to EM radiation from traditional microwave communication) frequency range and value of emissivity (ϵ) is taken from [31]. However, the values of the polarization factor are taken as less than one. Further, in order to keep the linking of the numerical discussion with the expressions derived in section II-A and section II-B, this section is divided into two subsections. In section III-A, PDF of RAN is discussed whereas, EP under RAN is analyzed in section III-B.

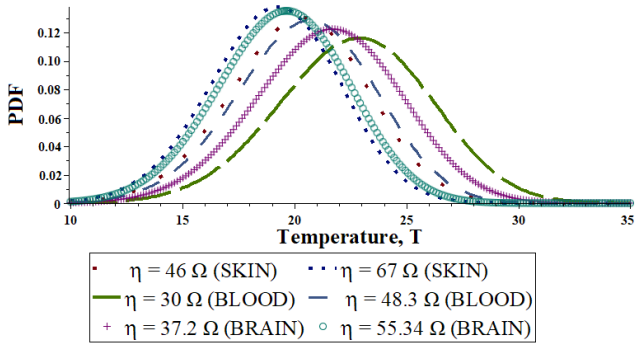

FIGURE 1. PDF of RAN in MHz frequency range with varying intrinsic impedance of body tissues for fixed polarization factor as $P_{13} = 0.001/P_{23} = 0.002$.

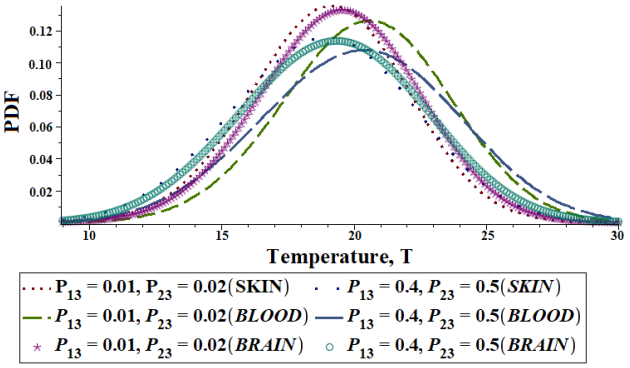

FIGURE 2. PDF of RAN in MHz frequency range with varying polarization factor under different body tissues at 400 MHz.

A. EFFECT OF DIFFERENT PARAMETERS ON THE PDF OF RAN

This subsection presents an analysis of the PDF of RAN proposed in section II-A, given by Eq. (15). First of all, the PDF of RAN is analyzed for the different sets of the intrinsic impedance of body tissues and polarization factors of incident EM wave in the MHz frequency range. Also, a similar analysis for PDF of RAN is presented in the THz frequency range. Finally, the comparison between PDF of RAN in MHz and THz frequency range respectively are discussed for the different values of the intrinsic impedance of body tissues.

Fig. 1, shows the PDF of radiation absorption noise for different tissues of the human body (skin, brain, and blood) as a function of temperature for different values of intrinsic the impedance of the tissues which depends on the frequency of incident EM wave However, the polarization factors P_{13} and P_{23} are kept constant. For skin, as the value of intrinsic impedance (η) increases from 46 Ω at 150 MHz to 67 Ω at 400 MHz, the peak of noise probability increases but shifted towards lesser temperature (left-hand side: LHS). This is so as, higher the value of the intrinsic impedance of the tissue lower the power density ($E_0{}^2/2\eta$) of incident EM wave. Therefore, a lesser rise in temperature is having a greater probability. Also, its vice-versa is true.

Similarly, as the value of intrinsic impedance increases from 30 Ω at 150 MHz to 48.3 Ω at 400 MHz and 37.2 Ω at 150 MHz to 55.34 Ω at 400 MHz for blood and brain respectively, the peak of noise probability shifted towards LHS. So, again as the value of the intrinsic impedance of the body tissue increases, the peak of noise probability increases but shifted towards LHS irrespective of the type of human body tissues. On the other hand, the inverse is also true.

However, for skin, the peak of noise probability is achieved at the least value of temperature whereas for blood it is achieved at the highest value of temperature at the given value of frequency (η of skin and blood are 67 Ω and 48.3 Ω at 400 MHz) as shown in Fig. 1. This observation clarifies that lower water content in the tissue results in lower conductivity and will give a higher value of intrinsic impedance as in [21, 28]. From Eq. (3) it can be observed that higher the value of the intrinsic impedance of the tissue implies in the lower power density of incident EM wave results in greater probability of the lesser rise in temperature as depicted in Fig.1.

Fig. 2, shows the effect of polarization factor of incident EM wave on the PDF of radiation absorption noise for different tissues of the human body like; skin, brain, and blood as a function of temperature. However, frequency is kept constant as 400 MHz that corresponds to the value of intrinsic impedances as 67 Ω, 48.3 Ω, and 55.34 Ω for skin, blood, and brain respectively. Also, values of polarization factor of incident EM wave are taken as $P_{13} = 0.01/\ P_{23} = 0.02$ and $P_{13} = 0.4/\ P_{23} = 0.5$. For skin, as the values of polarization factor increases from $P_{13} = 0.01/\ P_{23} = 0.02$ to $P_{13} = 0.4/\ P_{23} = 0.5$ the peak of noise probability decreases significantly for intrinsic impedance equal to 67 Ω at 400 MHz. This means that for a given tissue if the value of intrinsic impedance is fixed then a higher value of polarization factor of incident EM wave results in the lesser probability of the rise in temperature. Similarly, for blood and brain as the values of polarization factor increases from $P_{13} = 0.01/\ P_{23} = 0.02$ to $P_{13} = 0.4/\ P_{23} = 0.5$ the peak of noise probability again decreases. Though, the noticeable variation in the amplitude peak is different for them.

Also, from Fig. 2, it can be observed that for fixed frequency skin attains peak of the noise probability for least value of temperature as it has the highest value of intrinsic impedance at 400 MHz whereas, blood for highest value of temperature but peak of noise probability of brain lies between that of skin and blood.

Fig. 3, shows the effect of different tissues of the human body (skin, brain, and blood), polarization factor of incident EM wave, and intrinsic impedance of body tissue (which depends on the value of frequency of incident EM wave) on the PDF of radiation absorption noise as function of temperature. For skin, brain, and blood intrinsic impedances are 46 Ω, 37.199 Ω, and 30 Ω at 150 MHz and 67 Ω, 55.34 Ω, and 48.3 Ω at 400 MHz respectively.

Further, the polarization factors have been increased from $P_{13} = 0.001/P_{23} = 0.007$ to $P_{13} = 0.3/P_{23} = 0.6$ for

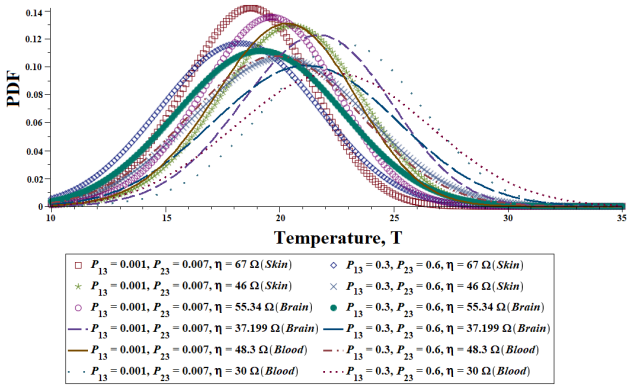

FIGURE 3. PDF of RAN in MHz frequency range under different body tissues at 150 MHz and 400 MHz for varying polarization factor.

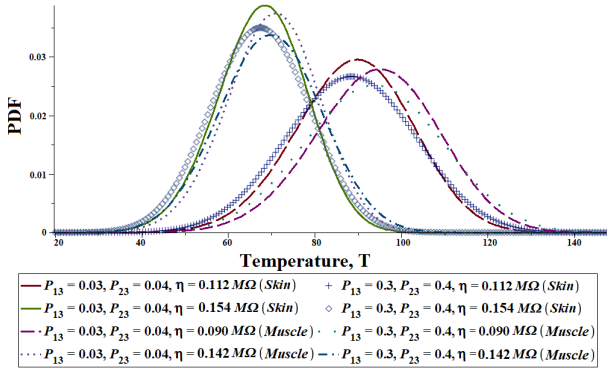

FIGURE 4. PDF of RAN in THz frequency range under different body tissues at 0.1 THz and 1 THz for varying polarization factor.

each value of intrinsic impedances of every tissue. For skin, at intrinsic impedance of 67 Ω, as polarization factors varies from $P_{13} = 0.001/P_{23} = 0.007$ to $P_{13} = 0.3/P_{23} = 0.6$, the noise peak decreases significantly but also shifted slightly towards LHS. Same is true at intrinsic impedance of 46 Ω, as polarization factors varies from $P_{13} = 0.001/P_{23} = 0.007$ to $P_{13} = 0.3/P_{23} = 0.6$. On the other hand, at fixed value of polarization factor, $P_{13} = 0.001/P_{23} = 0.007$ or $P_{13} = 0.3/P_{23} = 0.6$ as intrinsic impedance increases from 46 Ω to 67 Ω the peak of noise probability increases but shifted towards LHS. So, an increase in intrinsic impedance increases the noise peak but an increase in polarization factor decreases the noise peak. But either increase in intrinsic impedance or increase in polarization factor shifts the noise peak towards LHS. This shift is significant for an increase in intrinsic impedance but it is slight for an increase in polarization factor.

Now, for brain, at intrinsic impedance of 55.34 Ω, as polarization factors varies from $P_{13} = 0.001/P_{23} = 0.007$ to $P_{13} = 0.3/P_{23} = 0.6$, the noise peak decreases significantly but also shifted slightly towards LHS. Same is true at intrinsic impedance of 37.2 Ω, as polarization factors varies from $P_{13} = 0.001/P_{23} = 0.007$ to $P_{13} = 0.3/P_{23} = 0.6$. Further, at fixed value of polarization factor, $P_{13} = 0.001/P_{23} = 0.007$ or $P_{13} = 0.3/P_{23} = 0.6$ as intrinsic impedance increases from 37.2 Ω to 53.34 Ω the peak of noise PDF increases but shifted towards LHS. So, similar observation can be drawn for brain as it is drawn for skin for different variation in the parameters. Also, in Fig. 3 similar observations can be drawn for blood as well.

Further, it can be observed in Fig. 3 that for a fixed value of polarization factor as $P_{13} = 0.001/P_{23} = 0.007$ and fixed value of frequency at 150 MHz the intrinsic impedance of skin, brain, and blood are 46 Ω, 37.199 Ω, and 30 Ω respectively. The noise peak of the skin is achieved for the lowest value of temperature whereas for the blood the highest value of temperature is achieved, but for brain, it is in between the two. It is noteworthy to mention that all the assertions mentioned for Fig. 1 and Fig. 2 are equally valid and are also applicable for Fig. 3.

Finally, from Fig. 3 it is concluded that irrespective of body tissue; an increase in intrinsic impedance increases the peak of noise PDF but an increase in polarization factor decreases the noise peak, either increase in intrinsic impedance or increase in polarization factor shifts the noise peak towards LHS and the noise peak of skin is achieved for the lowest value of temperature whereas for blood it is achieved at the highest value of temperature, however for brain it is in between the two.

Finally, Fig. 4 concludes that irrespective of body tissue; an increase in intrinsic impedance increases the peak of noise PDF but an increase in polarization factor decreases the noise peak. Either an increase in intrinsic impedance or increase in polarization factor shifts the noise peak towards LHS. It is observed that the noise peak of the skin is achieved at the lowest value of temperature whereas the noise peak of muscle is achieved at the highest value of temperature for the given value of the polarization factor and frequency.

Further, this section discusses the comparison between PDF of RAN in MHz and THz frequency range drawn from Fig. 3 and Fig. 4 respectively for different values of the intrinsic impedance of skin. Though, in either case (either in MHz or in THz frequency range) the peak of noise probability increases but shifted towards lesser temperature (left-hand side: LHS) as intrinsic impedance (depends on the value of frequency and given by [27] and [21], [28] for THz and MHz respectively) increases and it's vice-versa. However, the effect is profound for THz compare to the MHz frequency range as expected.

B. EFFECT OF DIFFERENT PARAMETERS ON EP UNDER RAN

This subsection presents an analysis of EP under RAN proposed in section II-B, given by Eq. (26). First of all, EP under RAN is analyzed for a different set of the intrinsic impedance of body tissues and polarization factors of incident EM wave in the MHz frequency range. Also, a similar analysis for EP under RAN is presented in the THz frequency range. Finally, the comparison between EP under RAN in MHz and THz frequency range respectively are discussed for the different values of the intrinsic impedance of body tissues.

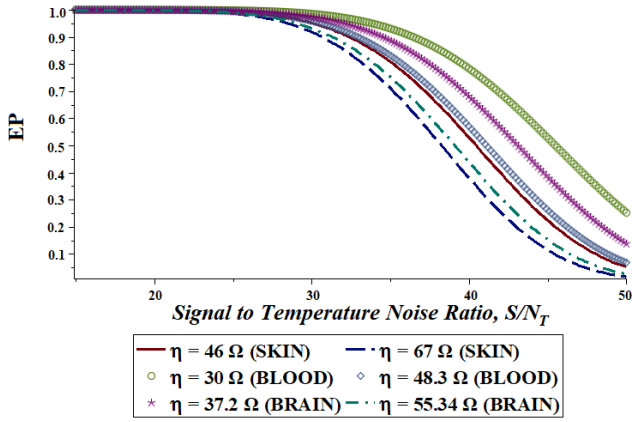

FIGURE 5. EP under RAN in MHz frequency range with varying intrinsic impedance of body tissues for fixed polarization factor as $P_{13} = 0.001/P_{23} = 0.002$.

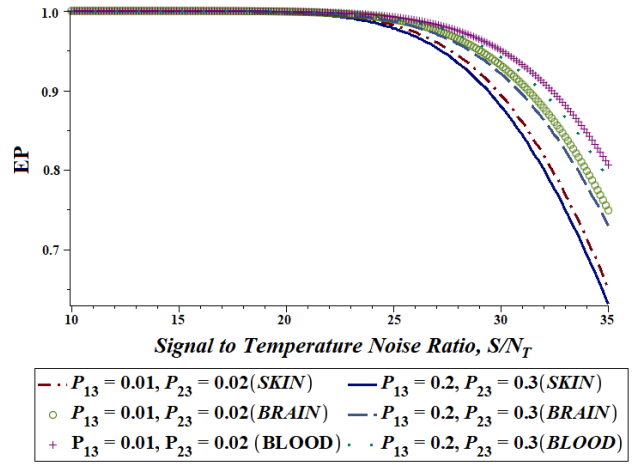

FIGURE 6. EP under RAN in MHz frequency range with varying polarization factor for different body tissues at 400 MHz.

Fig. 5 shows the EP of MNC under RAN for different human body tissues (brain, skin, blood) and intrinsic impedances keeping polarization factor fixed ($P_{13} = 0.001/P_{23} = 0.002$) as a function of SNR. For blood, an intrinsic impedance of 30 Ω which is lowest out of brain, skin, and blood at 150 MHz, results in the highest error probability. This is so as lower is the intrinsic impedance more is the probability of a larger rise in temperature and a larger rise in temperature contribute to more noise. Similar observations can be made from the curve of the brain with an intrinsic impedance of 37 Ω at 150 MHz, skin with an intrinsic impedance of 46 Ω at 150 MHz, blood with intrinsic impedance of 48.3 Ω at 400 MHz, brain with intrinsic impedance of 55.34 Ω at 400MHz and brain with intrinsic impedance of 67 Ω at 400 MHz. Finally, it can be concluded that for given SNR the error probability increases with decrease in intrinsic impedance from 67 Ω (skin) to 30 Ω (blood) as expected (lower is the intrinsic impedance more is the probability of a larger rise in temperature and larger a in temperature contribute to more noise).

Fig. 6 shows the EP under RAN for different values of polarization factor of incident EM wave, and for different

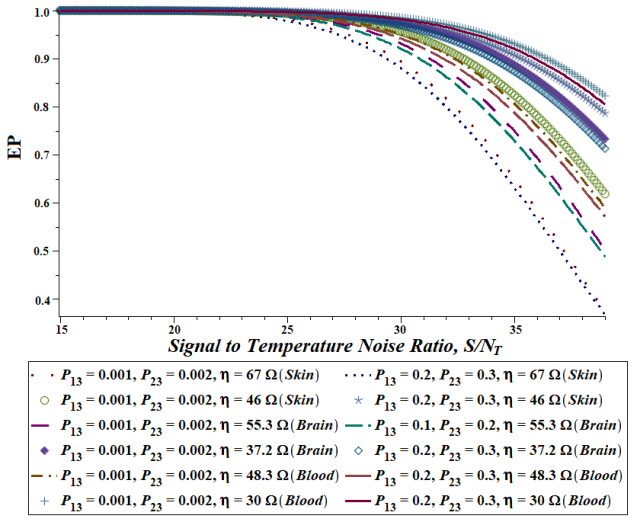

FIGURE 7. EP under RAN in MHz frequency range under different body tissues at 150 MHz and 400 MHz for varying polarization factor.

tissues of the human body (skin, brain, and blood) at 400 MHz as a function SNR. At 400 MHz the values of the intrinsic impedance of skin, brain, and blood are 67 Ω, 55.3 Ω, and 48.3 Ω respectively. For skin, as polarization factor increases from $P_{13} = 0.01/P_{23} = 0.02$ to $P_{13} = 0.2$ / $P_{23} = 0.3$ error probability decreases significantly for higher value of SNR. This is so as higher the value of polarization factor of incident EM wave lesser the probability of the rise in temperature and the hence lesser chance of noise. Also, for brain and blood, as polarization factor increases from $P_{13} = 0.01/P_{23} = 0.02$ to $P_{13} = 0.2$ / $P_{23} = 0.3$ a significant decrease in error probability is observed for higher value of SNR.

Further, from Fig. 6, for a fixed value of polarization factor (either $P_{13} = 0.01/P_{23} = 0.002$ or $P_{13} = 0.2$ / $P_{23} = 0.3$) blood has the lowest intrinsic impedance of 48.3 Ω and highest error probability whereas that for skin is minimum but for the brain is in between the two. This is so as the water content of blood is highest, and higher the water content higher the conductivity which results in lower intrinsic impedance [21], [28]. And from the previous paragraph lower the intrinsic impedance higher the chance of the rise in temperature which is noise for the system under consideration.

Fig. 7, shows the EP under RAN for different tissues of the human body (skin, brain, and blood), polarization factor of incident EM wave and intrinsic impedance of tissues as a function of SNR. For skin, brain, and blood the intrinsic impedances are 67 Ω, 48.3 Ω, and 55.3 Ω respectively at 400 MHz and are 46 Ω, 37.2 Ω, and 30 Ω respectively at 150 MHz. Further, the polarization factors is increased from $P_{13} = 0.001/P_{23} = 0.002$ to $P_{13} = 0.2/P_{23} = 0.3$ for each value of intrinsic impedances of every tissue.

It can be observed that for skin as polarization factor increases from $P_{13} = 0.001/ P_{23} = 0.002$ to $P_{13} = 0.2/P_{23} = 0.3$, the error probability decreases significantly for fixed value of intrinsic impedance as 67 Ω. Whereas, for either values of polarization factor, $P_{13} = 0.001/ P_{23} = 0.002$ or

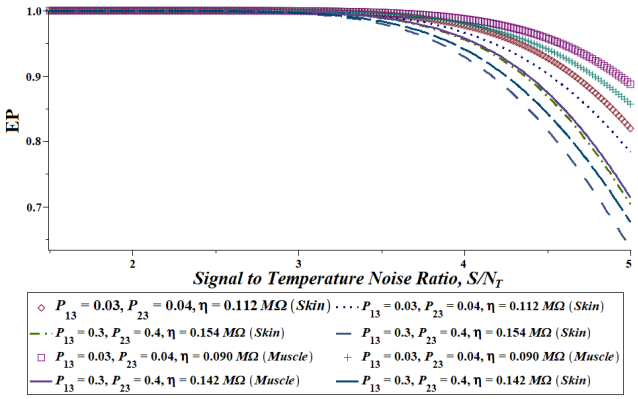

FIGURE 8. EP under RAN in THz frequency range for different body tissues at 0.1 THz and 1 THz for varying polarization factor.

$P_{13} = 0.2/P_{23} = 0.3$ as intrinsic impedance increases from 46 Ω to 67 Ω error probability decreases. Similar, observations can be drawn for brain and blood with respect to either increase in polarization factor or increase in intrinsic impedance.

Finally, it can be observed that for given polarization factor ($P_{13} = 0.001/\ P_{23} = 0.002$ or $P_{13} = 0.2/P_{23} = 0.3$) the error probability is lowest for skin and highest for blood, but it is in between for brain. Once, again it is noteworthy to mention that all the assertions mentioned for Fig. 5 and Fig. 6 are equally valid and applicable for Fig. 7.

Further, from Fig. 8 it can be observed that for skin, as polarization factor increases from $P_{13} = 0.03\ /\ P_{23} = 0.04$ to $P_{13} = 0.3\ /\ P_{23} = 0.4$ the error probability decreases significantly for fixed value of intrinsic impedance. Whereas, for fixed values of polarization factor ($P_{13} = 0.03\ /\ P_{23} = 0.04$ or $P_{13} = 0.3\ /\ P_{23} = 0.4$) as intrinsic impedance increases from 0.112 $M\Omega$ to 0.154 $M\Omega$ the EP decreases significantly. Similar, observations can be drawn for muscle with respect to either increase in intrinsic impedance or increase in polarization factor of incident EM wave. Finally, it can be observed that for given polarization factor ($P_{13} = 0.03\ /\ P_{23} = 0.04$ or $P_{13} = 0.3\ /\ P_{23} = 0.4$) and frequency, the error probability of skin is lower than that of muscle.

Finally, this section discusses the comparison between EP under RAN in MHz and THz frequency range drawn from Fig. 7 and Fig. 8 respectively for different values of the intrinsic impedance of skin. It may be noted that in either case (either in MHz or in THz frequency range) as intrinsic impedance (depends on the value of frequency and given by [27] and [28] for THz and MHz respectively) increases EP decreases. However, the effect is profound for THz compare to the MHz frequency range as expected.

IV. CONCLUSION

A novel noise model for MNC, due to increase in temperature by virtue of radiation absorption of incident EM energy by the tissues of the body, is modelled in this research paper. Analytical expressions of the probability density function of the noise and error probability under proposed noise are derived for MNC. It is found that for any of the tissues like skin, brain, and blood, the peak of noise probability is shifted towards LHS as the value of intrinsic impedance, which depends on frequency, increases. On the other hand, as the values of polarization factor increases, the peak of noise probability decreases significantly for a fixed value of intrinsic impedance. However, either increase in intrinsic impedance or increase in polarization factor shifts the noise peak towards LHS, but the noise peak of skin is achieved for the lowest value of temperature whereas blood for the highest value of temperature, but for the brain, it is in between the two. Further, in case of EP it is observed that for any of the tissue, as polarization factor increases, EP decreases significantly for a fixed value of intrinsic impedance. On the other hand, for any value of polarization factor as intrinsic impedance increases, EP decreases significantly. In place of considering equal transmission strategy, non-equal transmission strategy could be the future aspect of this work. In addition, the joint effect of different noises of MNC can be analysed in future work.

REFERENCES

[1] E. Balevi and O. B. Akan, "A physical channel model for nanoscale neuro-spike communications," *IEEE Trans. Commun.*, vol. 61, no. 3, pp. 1178–1187, Mar. 2013.

[2] D. Arifler, "Capacity analysis of a diffusion-based short-range molecular nano-communication channel," *Comput. Netw.*, vol. 55, no. 6, pp. 1426–1434, Apr. 2011.

[3] I. F. Akyildiz and J. M. Jornet, "Electromagnetic wireless nanosensor networks," *Nano Commun. Netw.*, vol. 1, no. 1, pp. 3–19, Mar. 2010.

[4] H. Elayan, P. Johari, R. M. Shubair, and J. M. Jornet, "Photothermal modeling and analysis of intrabody terahertz nanoscale communication," *IEEE Trans. Nanobiosci.*, vol. 16, no. 8, pp. 755–763, Dec. 2017.

[5] Y. Chahibi, "Molecular communication for drug delivery systems: A survey," *Nano Commun. Netw.*, vol. 11, pp. 90–102, Mar. 2017.

[6] Y. Chahibi and I. F. Akyildiz, "Molecular communication noise and capacity analysis for particulate drug delivery systems," *IEEE Trans. Commun.*, vol. 62, no. 11, pp. 3891–3903, Nov. 2014.

[7] R. Zhang, K. Yang, Q. H. Abbasi, K. A. Qaraqe, and A. Alomainy, "Analytical modelling of the effect of noise on the terahertz *in-vivo* communication channel for body-centric nano-networks," *Nano Commun. Netw.*, vol. 15, pp. 59–68, Mar. 2018.

[8] J. M. Jornet and I. F. Akyildiz, "Channel modeling and capacity analysis for electromagnetic wireless nanonetworks in the terahertz band," *IEEE Trans. Wireless Commun.*, vol. 10, no. 10, pp. 3211–3221, Oct. 2011.

[9] I. F. Akyildiz, J. M. Jornet, and M. Pierobon, "Nanonetworks: A new frontier in communications," *Commun. ACM*, vol. 54, no. 11, p. 84, Nov. 2011.

[10] M.-J. Moore, T. Suda, and K. Oiwa, "Molecular communication: Modeling noise effects on information rate," *IEEE Trans. Nanobiosci.*, vol. 8, no. 2, pp. 169–180, Jun. 2009.

[11] K. V. Srinivas, A. W. Eckford, and R. S. Adve, "Molecular communication in fluid media: The additive inverse Gaussian noise channel," *IEEE Trans. Inf. Theory*, vol. 58, no. 7, pp. 4678–4692, Jul. 2012.

[12] C. T. Chou, "Noise properties of linear molecular communication networks," *Nano Commun. Netw.*, vol. 4, no. 3, pp. 87–97, Sep. 2013.

[13] U. A. K. Chude-Okonkwo, S. Nunoo, and R. Ngah, "Diffusion-based molecular communication concentration and capacity dependencies on human body temperature variation," in *Proc. IEEE 10th Int. Colloq. Signal Process. Appl.*, Mar. 2014, pp. 53–57.

[14] S. Qiu, T. Asyhari, W. Guo, S. Wang, B. Li, C. Zhao, and M. Leeson, "Molecular channel fading due to diffusivity fluctuations," *IEEE Commun. Lett.*, vol. 21, no. 3, pp. 676–679, Mar. 2017.

[15] Y. A. Sambo, F. Heliot, and M. A. Imran, "A survey and tutorial of electromagnetic radiation and reduction in mobile communication systems," *IEEE Commun. Surveys Tuts.*, vol. 17, no. 2, pp. 790–802, Oct. 2014.
[16] K. H. Kim, E. Kabir, and S. A. Jahan, "The use of cell phone and insight into its potential human health impacts," *Environ. Monit. Assessment*, vol. 188, no. 4, p. 221, Apr. 2016.
[17] H. Elayan, C. Stefanini, R. M. Shubair, and J. M. Jornet, "End-to-end noise model for intra-body terahertz nanoscale communication," *IEEE Trans. Nanobiosci.*, vol. 17, no. 4, pp. 464–473, Oct. 2018.
[18] J. Xu, K. W. Plaxco, and S. J. Allen, "Absorption spectra of liquid water and aqueous buffers between 0.3 and 3.72THz," *The J. Chem. Phys.*, vol. 124, no. 3, Jan. 2006, Art. no. 036101.
[19] R. Zhang, K. Yang, A. Alomainy, Q. H. Abbasi, K. Qaraqe, and R. M. Shubair, "Modelling of the terahertz communication channel for *in-vivo* nano-networks in the presence of noise," in *Proc. 16th Medit. Microw. Symp. (MMS)*, Nov. 2016, pp. 1–4.
[20] G. Piro, K. Yang, G. Boggia, N. Chopra, L. A. Grieco, and A. Alomainy, "Terahertz communications in human tissues at the nanoscale for healthcare applications," *IEEE Trans. Nanotechnol.*, vol. 14, no. 3, pp. 404–406, May 2015.
[21] P. A. Hasgall, F. Di Gennaro, C. Baumgartner, E. Neufeld, B. Lloyd, M. C. Gosselin, D. Payne, A. Kligenbock, and N. Kuster. (May 15, 2018). *IT'IS Database for Thermal and Electromagnetic Parameters of Biological Tissues, Version 4.0*. [Online]. Available: https://itis.swiss/virtual-population/tissue-properties/database/, doi: 10.13099/VIP21000-04-0.
[22] P. Wang, J. M. Jornet, M. Abbas Malik, N. Akkari, and I. F. Akyildiz, "Energy and spectrum-aware MAC protocol for perpetual wireless nanosensor networks in the Terahertz Band," *Ad Hoc Netw.*, vol. 11, no. 8, pp. 2541–2555, Nov. 2013.
[23] C. Johnson, "Mathematical physics of blackbody radiation," in *Icarus iDucation Skolanfördataveten skapochkommunikation*. Sweden, Stockholm: Högskolan Kungliga Tekniska, 2012.
[24] L. Arnaut, "Compound exponential distributions for undermoded reverberation chambers," *IEEE Trans. Electromagn. Compat.*, vol. 44, no. 3, pp. 442–457, Aug. 2002.
[25] I. D. Flintoft, M. P. Robinson, G. C. R. Melia, A. C. Marvin, and J. F. Dawson, "Average absorption cross-section of the human body measured at 1–12 GHz in a reverberant chamber: Results of a human volunteer study," *Phys. Med. Biol.*, vol. 59, no. 13, pp. 3297–3317, Jul. 2014.
[26] I. D. Flintoft, G. C. R. Melia, M. P. Robinson, J. F. Dawson, and A. C. Marvin, "Rapid and accurate broadband absorption cross-section measurement of human bodies in a reverberation chamber," *Meas. Sci. Technol.*, vol. 26, no. 6, Jun. 2015, Art. no. 065701.
[27] L. Zilberti, D. Voyer, O. Bottauscio, M. Chiampi, and R. Scorretti, "Effect of Tissue Parameters on Skin Heating Due to Millimeter EM Waves," *IEEE Trans. Magn.*, vol. 51, no. 3, pp. 1–4, Mar. 2015.
[28] R. B. Schulz, V. C. Plantz, and D. R. Brush, "Shielding theory and practice," *IEEE Trans. Electromagn. Compat.*, vol. 30, no. 3, pp. 187–201, Aug. 1988.
[29] H. L. Van Trees, *Detection, Estimation, and Modulation Theory. Part I: Detection, Estimation, and Linear Modulation Theory*. Hoboken, NJ, USA: Wiley, 2004.
[30] J. G. Proakis, M. Salehi, N. Zhou, and X. Li, *Communication Systems Engineering*, vol. 2. Upper Saddle River, NJ, USA: Prentice-Hall, 1994.
[31] B. Jones and P. Plassmann, "Digital infrared thermal imaging of human skin," *IEEE Eng. Med. Biol. Mag.*, vol. 21, no. 6, pp. 41–48, Nov. 2002.

S. PRATAP SINGH (Member, IEEE) received the B.Tech. degree from RGPV, Bhopal, India, in 2003, the M.Tech. degree from TIET, Patiala, in 2010, and the Ph.D. degree in wireless communication from BIT, Mesra, Ranchi, India, in 2018. He has more than 14 years of experience in teaching and research. He is currently working as an Associate Professor with GCET, Greater Noida, India. He has filed one Indian IPR (patent) with application number TEMP/E-1/32775/2019-DEL. Two more IPR are under process. He has published more than 30 Scopus indexed research articles in IEEE conferences. He has also published six SCI research articles in reputed journals of *Springer, Taylors and Francis, Willey,* and *Inderscience*. His research interests are in modeling, analysis, and removal of various impairments in wireless communications and in nano communication systems. He is a member of GISFI and a Fellow of IETE.

SHEKHAR SINGH received the B.Tech. degree in electronics and communication engineering from Galgotias College of Engineering and Technology (GCET), Greater Noida, India, in 2019. His final year project is entitled as Channel Impairment Analysis in Nano Communication under CM-3 Scenario was published in SPIN 2019 (IEEE International Conference). Also, one Indian IPR (patent) is under process. His interest includes modeling of channel impairments in nano communication.

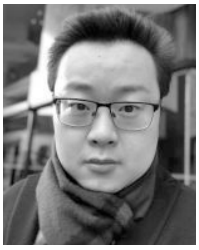

WEISI GUO (Senior Member, IEEE) received the M.Eng., M.A., and Ph.D. degrees from the University of Cambridge. He is currently working as a Professor with Cranfield University. He has published over 110 articles. He is also the PI on over 2.0 million pounds of research grants from EPSRC, H2020, and Innovate U.K. He is also the Coordinator of the H2020 Project: Data-Aware-Wireless-Networks for IoE. His research has received several international awards (IET Innovation 15, Bell Labs Prize Finalist 14, and Semi-Finalist 16) and a Turing Fellowship from The Alan Turing Institute.

SAKET MISHRA received the B.Tech. degree in electronics and communication engineering from GCET, India, in 2017. He is currently working with IBM India Pvt., Ltd., as an Infrastructure Specialist Administrator on cloud services. He has achieved first position in J. N. National Science Exhibition at State level for Renewable Energy Project. His research interests include nano communication and cognitive cloud technology.

SANJAY KUMAR received the M.Tech. degree in electronics and communication engineering from the Guru Nanak Dev Engineering College, Ludhiana, in 2000, and the Ph.D. degree in wireless communication from Aalborg University, Denmark, in 2009. He has about 33 years of teaching, research, and work experience in the field of wireless communication. He has been closely associated with organizing, reviewing, and contributing to several conferences and workshops. He is currently working as an Associate Professor with the Department of Electronics and Communications Engineering, Birla Institute of Technology, Mesra, Ranchi, India. He has contributed above 80 research articles in various National and International journals and conferences in the field of wireless communication. He has also contributed a chapter in the book *New Directions in Wireless Communications Research* (USA, Springer, 2009). His book *Wireless Communication: The Fundamental and Advanced Concepts* (Denmark, 2015). He is a Fellow of IETE, India, a Senior Member of the Institution of Communication Engineers and Information Technologists, a member of the Institution of Engineers, India, and a Life Member of ISTE and GENCO Alumni Association, and Guru Nanak Dev Engineering College, Ludhiana, India.

https://dspace.org/

Radiation absorption noise for molecular information transfer

Singh, S. Pratap; Singh, Shekhar; Guo, Weisi; Mishra, Saket; Kumar, Sanjay

2020-01-01
IEEE
https://doi.org/10.1109/ACCESS.2019.2963485
Pratap Singh S, Singh S, Guo W. (2020) Radiation absorption noise for molecular information transfer. IEEE Access, Volume 8, 2020, pp. 6379-6387

Downloaded from a DSpace repository. https://dspace.org/